


Direct ultrasonic evidence for heterophase oscillations near the 186 K transition in KMnF_3 Jean Toulouse ^{*}*Physics Department, Lehigh University, Bethlehem, Pennsylvania 18015, USA* (Received 22 October 2023; revised 3 January 2024; accepted 16 January 2024; published 12 February 2024)

KMnF_3 is one of the first systems in which a dynamic “central peak” was observed by inelastic neutron scattering in the vicinity of a structural phase transition. The origin of this peak, however, whether intrinsic or extrinsic, was never fully resolved. In the present paper, we report combined dielectric and ultrasonic results on KMnF_3 , pure and lightly doped with lithium, which provide direct evidence for the presence of intrinsic “heterophase (cubic-tetragonal) oscillations” near the transition. These oscillations are seen as a “second sound” wave, akin to the density wave observed in liquid helium near the superfluidity transition.

DOI: [10.1103/PhysRevB.109.064103](https://doi.org/10.1103/PhysRevB.109.064103)**I. INTRODUCTION**

KMnF_3 is one of the first systems along with SrTiO_3 in which a dynamic “central peak” (CP) was observed many years ago in the inelastic neutron scattering spectra [1]. In KMnF_3 , this peak was found to appear almost 40 K above the transition, growing in intensity and narrowing down in width as the transition was approached, eventually becoming subsumed into the elastic peak close to the transition. It was attributed to overdamping of the soft zone-boundary mode by critical precursor fluctuations with a frequency-dependent damping [2]. Later x-ray diffraction studies revealed the presence of two critical elastic scattering peaks, a narrow quasi-Bragg peak and a broad Lorentzian squared one, corresponding respectively to two different length scales [3]. The narrow peak was prominent in thin samples and appeared to originate from the region near the surface while the broad peak (corresponding to a short length scale) originated in the bulk but was not observed in all crystals and therefore possibly related to defects (extrinsic).

To this day, however, there is no general agreement as to the origin of the central peak or the nature of these two length scales, although there seems to be a consensus that strain fields play an important role. This question is still of current interest, as precursor fluctuations can be responsible for very large susceptibilities near phase transitions and may explain the behavior of a broad class of condensed matter systems.

In the present paper, we report dielectric and ultrasonic results on KMnF_3 , pure and doped with lithium, that reveal the existence of “heterophase dynamics” near the phase transition, which should therefore also be responsible for the dynamic CP observed in inelastic neutron scattering and for the broad diffraction peak in x-ray studies. The similar results obtained in pure and Li-doped crystals suggest that the observed dynamics is an intrinsic feature of this type of structural transition, which can nevertheless be modified by dopants. The nature of the ultrasonic evidence for these intrinsic precursor dynamics also suggests an analogy with “second sound” observed near the transition of helium from a normal to a superfluid liquid.

II. EXPERIMENTAL DETAILS AND RESULTS

The four crystals used in this study were grown in Le Mans (France) by the Bridgman technique. One of them was nominally pure and the other three doped with lithium. The starting materials were optical purity MnF_2 crystals and high-purity KF powder. Doping was done in the melt with an appropriate addition of LiF. As determined by several atomic absorption analyses, the concentrations of lithium in the three doped crystals were found to be 1221 ppm (nominal concentration 1%), 1338 ppm, and 8700 ppm, respectively. The samples for the dielectric measurements were obtained by cleavage from clear sections of the boules and did not show signs of a strong mosaicity. They were polished and coated with painted silver electrodes and mounted in pairs in a sample holder that was then placed in a Janis Superveritemp dewar. A silicon diode temperature sensor was affixed with silver paint directly onto the sample holder and close to the sample. The measurements were made at successive temperatures, after sufficient equilibration times at each temperature for the capacitance to remain constant (approximately 5 min with 2° temperature changes outside of the critical region, and up to ≈30 min with temperature changes of 0.01°–0.04° in the critical region of the temperature hysteresis loop). The capacitance was measured with a General Radio bridge (model 1615A) at 1 kHz. Finally, but most importantly, in order to compare the transition temperatures of the different samples despite the small shifts involved, different *pair combinations of samples* were measured in each low-temperature run. The normalized dielectric constant, $\epsilon(T)/\epsilon(295\text{ K})$, is shown in Fig. 1 [$\epsilon(295\text{ K}) = 8.75 \pm 0.15$]. The normalization allowed us to eliminate the uncertainty related to electrode geometry.

At high temperature, the dielectric constant is found to increase linearly with decreasing temperature for all four samples. Approximately 45 K from the transition, it departs from this linear dependency, with the largest deviation observed for the pure crystal, and being less pronounced the higher the lithium concentration. This suggests that the departure of the dielectric constant from a linear dependence is an intrinsic characteristic of the pure system, only being modified by the introduction of the lithium impurities. Although not

^{*}jt02@lehigh.edu

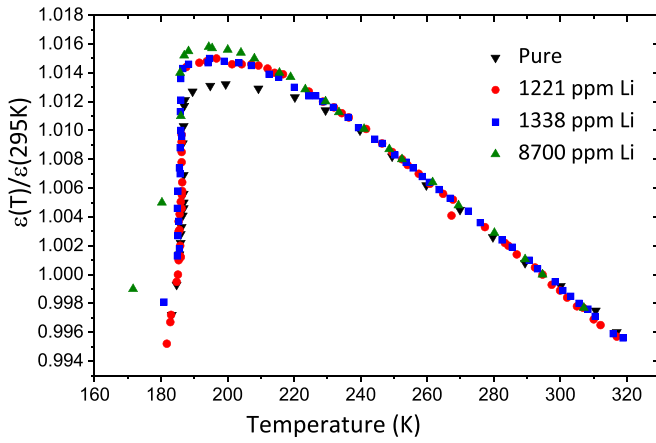


FIG. 1. Dielectric constant vs temperature for KMnF_3 crystals with three different Li concentrations.

a ferroelectric, KMnF_3 exhibits a drop in dielectric constant at its 186 K structural transition and a very narrow thermal hysteresis loop (Fig. 2). The transition is therefore weakly first order. The drop in the dielectric constant upon approaching the transition was reported earlier [4] and attributed to a strong interaction between the soft R_{25} mode and the acoustic modes in both KMnF_3 and SrTiO_3 , and the condensation of the former as a new zone center mode [5]. In order to show the four hysteresis loops on the same graph and compare their shapes, an arbitrary but different quantity Y was subtracted from each of the ratios plotted in Fig. 1. Such a subtraction does not affect the size or shape of the hysteresis loop. In Fig. 2, lithium is seen to lower the transition temperature slightly (see the horizontal scale ≤ 1 K) and compress the hysteresis loop (narrower width and sharper drops) for the two lower concentrations. The temperature ordering of the hysteresis loops suggests that the lithium impurities retard the onset of the critical fluctuations, and even suppress them for the highest concentration (8700 ppm). The higher concentration

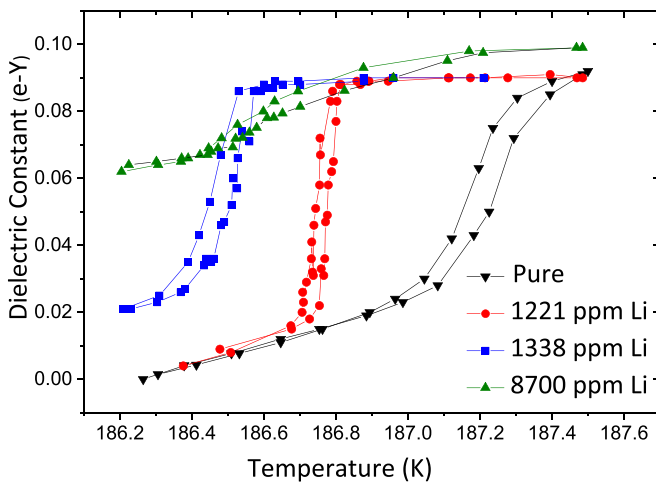


FIG. 2. Dielectric constant vs temperature for the same crystals as in Fig. 1 in the narrow region of the thermal hysteresis around the phase transition.

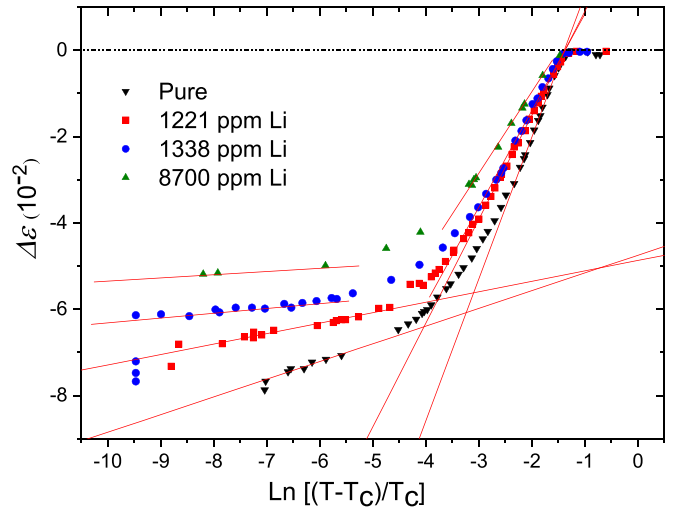


FIG. 3. Deviation of the dielectric constant from a linear dependence vs $\ln \tau$.

loop is stretched and flattened, possibly indicating a nearby tricritical point [6].

To look more closely at the precursor effects, in Fig. 3 we have extracted the critical part $\Delta\epsilon$ by subtracting the measured ϵ values from the extrapolated high-temperature linear dependence. Because it appears to reveal a characteristic critical behavior not apparent otherwise, in that figure $\Delta\epsilon$ is plotted as a function of $\ln \tau$, with $\tau \equiv (T - T_c)/T_c$ a normalized temperature. A physical justification for this dependence is given later in the paper. The advantage of a normalized temperature is that it allows a direct comparison of the critical behavior in the different crystals, irrespective of their particular concentration and transition temperature. Several common features of the dielectric constant curves of Fig. 1 can be noted in Fig. 3: (i) The dielectric constant deviates from its high-temperature linear dependence at the same normalized temperature for all four crystals, $\tau = 0.25$, which corresponds to $(T - T_c) \approx 45$ K and (ii) two stages are observed in the critical behavior, both proportional to $\ln[(T - T_c)/T_c]$ but with different slopes. It is worth noting that the dynamic central peak observed in neutron scattering also appears approximately 45° above the transition and that the soft mode has vanished into the central peak below $\sim T_c + 2$ K (or $\ln[(T - T_c)/T_c] \sim -4.5$) [1], i.e., in the lower-temperature region of Fig. 3.

To further investigate the precursor dynamics, ultrasonic measurements were carried out using the pulse-echo method. The ultrasonic measurements were performed with a partially home-assembled system based on separate units from Ritec, Incorporated. The system used a superheterodyne detection stage providing both the in-phase and quadrature components of the signal. A detailed description of the system can be found in Ref. [7]. The crystals used were approximately $1 \times 1 \times 1.7$ cm. Opposite faces normal to the long dimension of the crystal were polished with a special holder to an optical ($\lambda/20$) finish and the flatness and parallelism of the faces were checked interferometrically. These last two steps were crucial in allowing precise ultrasonic measurements and the observation of the phenomenon described below. A longitudinal

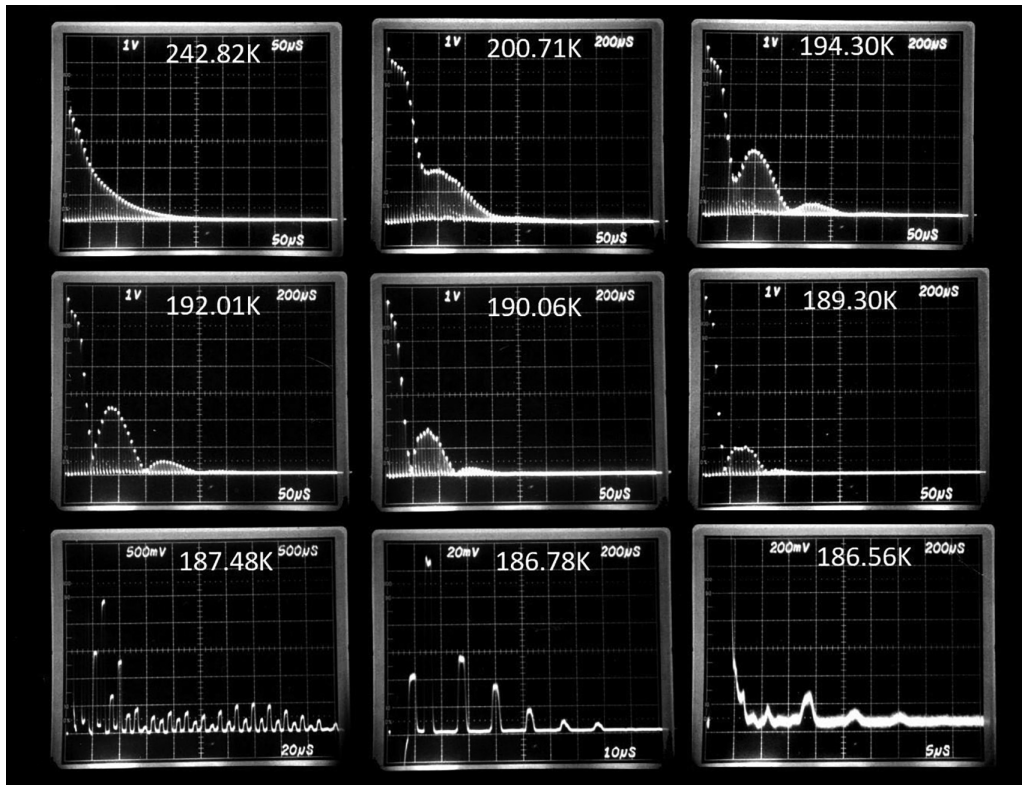


FIG. 4. Echo decay in the $\text{KMnF}_3 : 1\% \text{Li}$ (1221 ppm) crystal.

quartz transducer with concentric gold electrodes was affixed onto the crystal with Nonaq grease and the sample and transducer were placed in a specially designed spring-loaded sample holder that allowed for electrical contacts. The echo trains were recorded after the temperature had been equilibrated and when they had been stable for the same lengths of time as indicated above for the dielectric constant measurements. It is worth emphasizing that our temperature equilibration times for both the dielectric and ultrasonic measurements were identical or even exceeded those reported in corresponding studies (see Stokka *et al.* [8], 12 mK temperature steps and 5 min equilibration times at each point), especially in the critical range of the hysteresis (see the above dielectric results).

Traces of the echo trains in the $\text{KMnF}_3 : 1\% \text{Li}$ crystal are shown in Fig. 4 at different temperatures approaching the transition at ~ 186.7 K. The timescale on the horizontal axis of each oscilloscope trace is found on the lower right of each screen picture. In the precursor region identified above ($T < T_c + 45$ K), a clear modulation of the echo train develops, resulting in the appearance of successive zeros at progressively earlier echoes as the transition temperature is approached. However, all echoes are visible down to 187.48 K, although the odd echoes at that temperature are now clearly suppressed. Eventually, at 186.78 and 186.56 K, i.e., within the hysteresis loop, all the odd echoes have disappeared except for the first echo which appears only weakly. It should be noted that the very first pulse on each picture corresponds to the driving pulse imparted to the transducer and is therefore not an echo. The next pulse is the first echo.

Similar observations were also made at other frequencies (e.g., 75 MHz). At this point, it is worth mentioning that

other ultrasonic studies of KMnF_3 or SrTiO_3 did not present echo decays, either because the pulse echo or wave vector reversed echo technique was used [9,10], or because the echo decays were simply assumed to be distorted. Fossheim *et al.* [9] nevertheless pointed to missing echoes due to destructive interference in the critical temperature region. Hence, these authors did not report or analyze the modulation of the echo trains which is the focus of the present paper.

Now comparing the ultrasonic and dielectric results for the $\text{KMnF}_3 : 1\% \text{Li}$ crystal, the odd ultrasonic echoes are seen to be missing within precisely the temperature range of the thermal hysteresis in the dielectric results, i.e., a region in which both cubic and tetragonal phases can coexist. Although we have chosen to primarily feature the results for the 1%Li crystal because of their particular clarity, similar results were also observed in the pure KMnF_3 crystal. A few of the echo decays measured on the pure crystal in the transition range are shown in Fig. 5. They also show the appearance of zeros in the precursor region and, close to the transition and within the temperature range of the thermal hysteresis loop in the dielectric curve, the disappearance of all odd echoes at 187.64 and 186.78 K. Details of the missing echoes are shown in Fig. 6. Thus, these precursor effects are not simply related to the presence of defects but seem to be intrinsic to the KMnF_3 system and related to the transition itself. As a matter of fact, the stronger departure of the dielectric constant from a high-temperature linear temperature dependence in Fig. 1 suggests that these precursor effects are actually even more pronounced in the pure crystal.

The completeness and regularity of the successive zeros in Figs. 4, 5, and 6 suggests destructive interference between

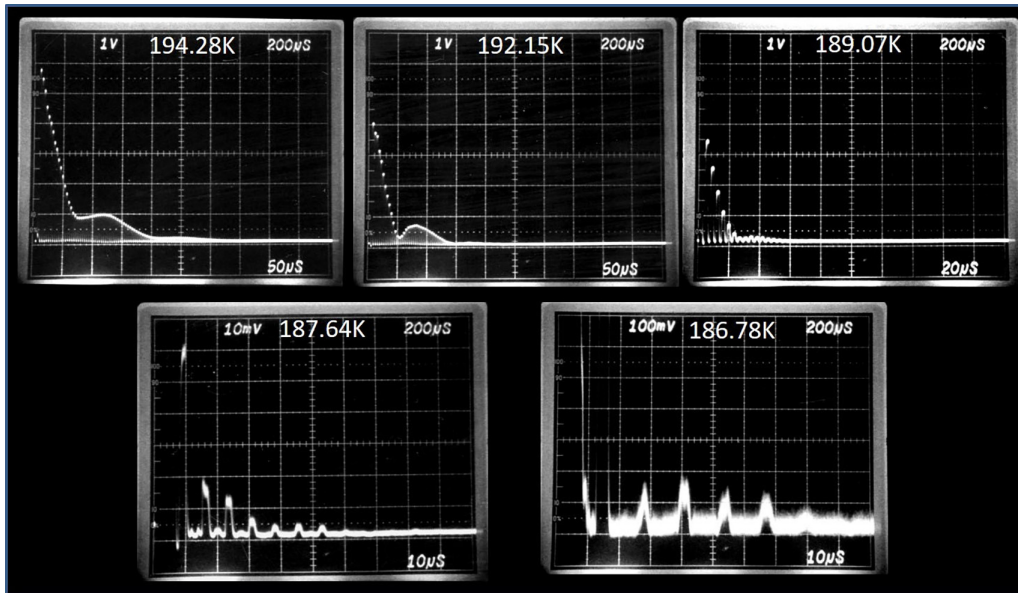


FIG. 5. Echo decay in the KMnF_3 pure crystal.

two waves, the primary sound wave and a secondary wave coherently excited by it along their common travel path through the crystal as it approaches the transition from above. Such a transition, from a cubic to a tetragonal phase, can be induced by the pressure (stress) from the primary sound wave, giving

rise to the coherently generated secondary wave that is naturally associated with *heterophase oscillations* between the two phases in the vicinity of the transition. As the tetragonal phase becomes progressively more stable near the transition, the velocity of the heterophase wave, or equivalently the frequency of the heterophase oscillations, will decrease and the phase difference between the two waves correspondingly will increase, as seen by progressively earlier zeros in the echo train. Comparing the dielectric and ultrasonic results shows that, in the critical region of the temperature hysteresis of the dielectric curves, all odd ultrasonic echo pulses have vanished in the echo train. This strongly supports the above interpretation of associating the secondary wave with coherent heterophase fluctuations driven by the primary sound wave. Such a secondary wave has been reported in other solids near their phase transition Ref. [11] but is most prominent in the transition region of liquid helium [12].

In liquid helium, this second sound corresponds to a density wave or thermal oscillations of the liquid between its normal and superfluid phases, or more exactly to the wavelike motion of the two fluids relative to or against each other. The effect observed here can similarly be attributed to a secondary wave of oscillations between the cubic and tetragonal phases excited by the primary sound (pressure) wave. Here, however, the oscillations are coherent because they are driven by the primary sound wave. When the primary and secondary waves reaching back to the transducer are π out of phase, the corresponding echo is canceled (destructive interference) and therefore absent from the echo train. Hence, at successive zeros, the phase difference between the primary and secondary wave must be such that

$$\Delta\phi = 2\pi\nu * m(t_{rt1} - t_{rt2}) = (2n + 1) * \pi, \quad (1)$$

FIG. 6. Destructive interference between the primary and secondary pulse for every odd echo after the first one; (top) KMnF_3 : 1%Li, (bottom) KMnF_3 pure.

i.e., an odd number of π , where $t_{rt} = 2L/v$ designates the round-trip time for each of the two waves, L is the length of the crystal, and m the number of the zeroed echo. The round-trip

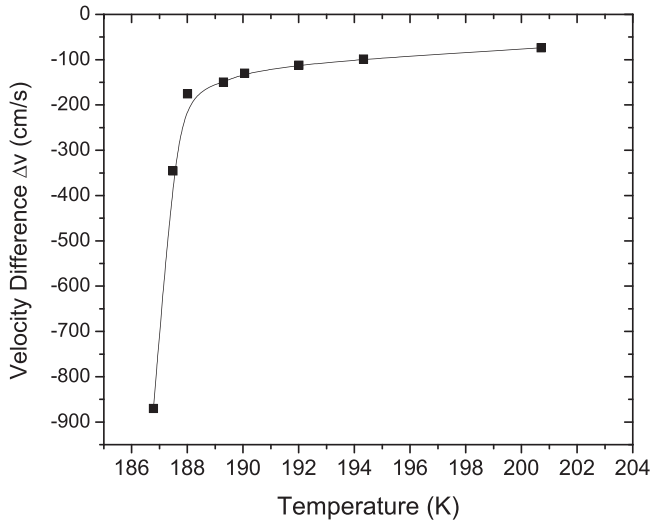


FIG. 7. Velocity difference between the primary and secondary waves.

time difference can thus be written as

$$(t_{r11} - t_{r12}) = 2L * (1/v_1 - 1/v_2) \approx 2L * \Delta v / v_1^2, \quad (2)$$

where the final approximation is justified below by the numerical values obtained. It is easy to see that successive zeros at a given temperature correspond precisely to successively higher values of n in Eq. (1), i.e., increasing dephasing between the two waves at each round trip. For instance, in Fig. 4 at 194.3 K the first zero (or minimum) is found between echoes 9 and 10. Using $m = 9.5$ and the measured round-trip time (1.575×10^{-3} s) to estimate v_1 , we calculate $\Delta v = 99.35$ cm/s, which is much smaller than either velocity and thus justifies the above approximation. This value can then be used to predict the next two zeros at echoes 28.5 and 47.5, in very good agreement with their observed positions (28 and 48).

In Fig. 7, Δv is plotted as a function of temperature. It is seen to be negative and becoming increasingly so as the transition is approached. This indeed corresponds to the evolution of the zeros on the echo trains, moving progressively closer to the time origin and closer to one another, revealing the increased phase difference between the two waves upon approaching the transition, so that fewer round trips of the primary wave result in the destructive interference of the two waves and the cancellation of the odd echoes. Since the round-trip time of the primary wave only decreases moderately with decreasing temperature, as can be seen in the echo spectrum, the (critical) slowing down must be attributed to the secondary wave. The final point on the graph, at $T = 186.78$ K, corresponds to $\Delta v = 870$ cm/s. In this tempera-

ture range all odd numbered echoes are missing, indicating a π phase difference per round trip between the primary and secondary waves. Even numbered echoes do appear because they correspond to a 2π phase difference between the two waves.

In another set of measurements, we also checked the frequency dependence of the zeroed echo numbers and found them to be in approximately the ratio of the frequencies as expected from Eq. (1) (see Table I). The small variation in the ratio of the frequencies is due to the fact that the quality of the destructive interference is very sensitive to the alignment of the transducer and the quality of the Nonaq bond, which was slightly lower for the pure crystal.

III. DISCUSSION AND ANALYSIS

The results presented above confirm the existence of a precursor temperature region and precursor effects within this region, as had been reported earlier in x-ray and neutron scattering studies on the basis of a central peak [1,13]. We observe the deviation of the dielectric constant from its linear high-temperature dependence and a modulation in the ultrasonic echo train in precisely the same temperature region in which a central peak was observed. The results presented here seem to indicate that these precursor effects are intrinsic to KMnF_3 , due to local oscillations between the high-temperature cubic and low-temperature tetragonal, and not due to defects. The deviation of the dielectric constant is indeed largest for pure KMnF_3 and the same modulation of the ultrasonic echo train is present in both pure and Li-doped KMnF_3 . The dielectric results presented would in fact suggest that lithium tends to suppress the precursor effects, leading to a smaller deviation from the linear high-temperature dependence, slightly lower transition temperatures, and narrower/sharper hysteresis loops. According to the defect nomenclature of Halperin and Varma [14], these observations would indicate that the lithium is a relaxing defect which, because of its small size, is often found in one of several interstitial positions between which it can reorient.

A dielectric relaxation peak was in fact observed for lithium doped into KZnF_3 , a perovskite system that is very similar to KMnF_3 , but with no phase transition. A corresponding dielectric relaxation peak could not be observed in KMnF_3 , being predicted to occur below the transition. If the dielectric results reveal the onset of critical fluctuations starting at $T_c + 45$ K, the modulation of the ultrasonic echo train suggests that these fluctuations can be driven into coherent oscillations by a sound wave with which

TABLE I. Comparison of zeroed echo numbers at two different frequencies in pure KMnF_3 .

Temperature (K)	No. zero echo 45 MHz	No. zero echo 75 MHz	Ratio 75/45 = 1.67
196.2	17	12	1.42
194.5	16	10	1.60
193.2	14	9	1.56
191.1	10	6	1.67
187.9	Odd echoes not yet missing	Odd echoes missing	

they can then interfere. In the past, such fluctuations have been called *heterophase oscillations* because they correspond to fluctuations of the system between a high-temperature and a low-temperature phase [15], here cubic and tetragonal. In the present case, they are driven coherently by the primary sound wave with which they can then interfere.

We now discuss the physical basis for the logarithmic divergence of the critical part of the dielectric constant. Logarithmic divergences are observed primarily near two-dimensional XY transitions where the broken symmetry variable is an angle, e.g., the orientation of the spins in the xy plane for a magnetic transition or the phase in superfluidity. Such transitions are explained theoretically by the Kosterlitz-Thouless theory [16]. This may indeed correspond to the case of KMnF_3 , where the order parameter is the rotational angle of the oxygen octahedron, which can be described as a pseudospin. The change of slope of the $\Delta\epsilon$ curve in Fig. 3 can be attributed to a change of regime of the critical phenomena. It is interesting to note that this change of slope corresponds to the onset of the precipitous drop (or negative increase) in Δv seen in Fig. 7 around 189 K, i.e., approximately 2.5 K above the transition. It may be useful to compare these results with those of an electron paramagnetic resonance (EPR) study of RbCaF_3 [17,18] which provided evidence for critical static fluctuations in the tetragonal phase, precursor order clusters in the $T_c - (T_c + 2 \text{ K})$ range, and a disordered high-temperature phase. The change in critical behavior seen in the present KMnF_3 results can be attributed to a crossover from dynamic to quasistatic fluctuations. This

is quite consistent with the fact that this change occurs within the thermal hysteresis loop observed in the dielectric results, and therefore within the narrow $\sim 2 \text{ K}$ two-phase transition region. Finally, these results also provide an explanation for the central peaks (CPs) reported in neutron scattering studies on this and other systems near structural phase transitions. Very close to the transition, and in the temperature region of our dielectric hysteresis, this CP is found to diverge in amplitude and its width to fall within the elastic scattering peak [1,2].

To answer the question stated at the beginning of this paper, in this latter region our results seem to indicate that this central peak is intrinsic, not primarily caused by impurities, and due to coherently driven heterophase oscillations between the high-temperature cubic and low-temperature tetragonal phase of KMnF_3 . Finally, one should expect such heterophase oscillations to be present in any system that undergoes a first-order transition and therefore exhibits a temperature region in which two phases can coexist and be switched under pressure [8,19].

ACKNOWLEDGMENT

We wish to thank M. Rousseau and P. Daniel of the University of Le Mans (France) for supplying the crystals for this study and for useful suggestions in interpreting the experimental results. The present study followed from earlier work on KMnF_3 initially funded by a grant from the Department of Energy, DE-FG02-86ER-45258.

-
- [1] S. M. Shapiro, J. D. Axe, G. Shirane, and T. Riste, *Phys. Rev. B* **6**, 4332 (1972).
 - [2] A. Gibaud, H. You, S. M. Shapiro, and J. Y. Gesland, *Phys. Rev. B* **42**, 8255 (1990).
 - [3] K. Hirota, J. P. Hill, S. M. Shapiro, G. Shirane, and Y. Fujii, *Phys. Rev. B* **52**, 13195 (1995).
 - [4] K. Rittenmyer, A. Bhalla, and L. Cross, *Ferroelectr. Lett. Sect.* **9**, 161 (1989).
 - [5] V. J. Minkiewicz and G. Shirane, *J. Phys. Soc. Jpn.* **26**, 674 (1969).
 - [6] S. Stokka, K. Fossheim, and V. Samulionis, *Phys. Rev. Lett.* **47**, 1740 (1981).
 - [7] J. Toulouse and J. C. Launay, *Rev. Sci. Instrum.* **59**, 492 (1988).
 - [8] S. Stokka and K. Fossheim, *J. Phys. C: Solid State Phys.* **15**, 1161 (1982).
 - [9] K. Fossheim and B. M. Holt, *Phys. Rev. Lett.* **45**, 730 (1980); J. O. Fossum and K. Fossheim, *J. Phys. C: Solid State Phys.* **18**, 5549 (1985).
 - [10] W. Cao and G. R. Barsch, *Phys. Rev. B* **38**, 7947 (1988).
 - [11] M. Chester, *Phys. Rev.* **131**, 2013 (1963).
 - [12] C. C. Ackerman, B. Bertman, H. A. Fairbanks, and R. A. Guyer, *Phys. Rev. Lett.* **16**, 789 (1966).
 - [13] I.-K. Jeong, T. W. Darling, J. K. Lee, T. Proffen, R. H. Heffner, J. S. Park, K. S. Hong, W. Dmowski, and T. Egami, *Phys. Rev. Lett.* **94**, 147602 (2005).
 - [14] B. I. Halperin and C. M. Varma, *Phys. Rev. B* **14**, 4030 (1976).
 - [15] J. Frenkel, *Kinetic Theory of Liquids* (Clarendon Press, Oxford, UK, 1946).
 - [16] J. M. Kosterlitz and D. J. Thouless, *J. Phys. C: Solid State Phys.* **6**, 1181 (1973).
 - [17] P. Simon, J. J. Rousseau, and J. Y. Buzare, *J. Phys. C: Solid State Phys.* **15**, 5741 (1982).
 - [18] C. Ridou, M. Rousseau, P. Daniel, J. Nouet, and B. Hennion, *Ferroelectrics* **124**, 293 (1991).
 - [19] R. M. Holt and K. Fossheim, *Phys. Rev. B* **24**, 2680 (1981).